Accepted Manuscript

The Fabrication of a Bifunctional Oxygen Electrodes without Carbon Components for Alkaline Secondary Batteries

Stephen W.T. Price, Stephen J. Thompson, Xiaohong Li, Scott F. Gorman, Derek Pletcher, Andrea E. Russell, Frank C. Walsh, Richard G.A. Wills

PII: S0378-7753(14)00251-1

DOI: 10.1016/j.jpowsour.2014.02.058

Reference: POWER 18721

To appear in: *Journal of Power Sources*

Received Date: 3 December 2013

Revised Date: 5 February 2014

Accepted Date: 15 February 2014

Please cite this article as: S.W.T. Price, S.J. Thompson, X. Li, S.F. Gorman, D. Pletcher, A.E. Russell, F.C. Walsh, R.G.A. Wills, The Fabrication of a Bifunctional Oxygen Electrodes without Carbon Components for Alkaline Secondary Batteries, *Journal of Power Sources* (2014), doi: 10.1016/j.jpowsour.2014.02.058.

The Fabrication of a Bifunctional Oxygen Electrodes without Carbon Components for Alkaline Secondary Batteries

Stephen W.T. Price[a], Stephen J. Thompson[a], Xiaohong Li[b], Scott F. Gorman[b],

Derek Pletcher[a], Andrea E. Russell[a], Frank C. Walsh[b], Richard G.A. Wills[b],

[a] *Chemistry, University of Southampton, Southampton, SO17 1BJ, UK*

[b] *Energy Technology Group, University of Southampton, Southampton, SO17 1BJ, UK*

The fabrication of a gas diffusion electrode (GDE) without carbon components is described. It is therefore suitable for use as a bifunctional oxygen electrode in alkaline secondary batteries. The electrode is fabricated in two stages (a) the formation of a PTFE-bonded nickel powder layer on a nickel foam substrate and (b) the deposition of a $NiCo_2O_4$ spinel electrocatalyst layer by dip coating in a nitrate solution and thermal decomposition. The influence of modifications to the procedure on the performance of the GDEs in 8 M NaOH at 333 K is described. The GDEs can support current densities up to 100 mA cm^{-2} with state-of-the-art overpotentials for both oxygen evolution and oxygen reduction. Stable performance during > 50 successive, 1 hour oxygen reduction/evolution cycles at a current density of 50 mA cm^{-2} has been achieved.

***Keywords*:** Carbon free gas diffusion electrode (GDE), bifunctional electrode, oxygen evolution/reduction.

1. Introduction

A successful renewable energy economy will require energy storage to manage the time differences between generation and customer demand. One solution is offered by flow batteries [1-3] although none of the systems extensively studied offer ideal behaviour and economics. Secondary metal/air batteries, particularly zinc/air [4-6], merit development. In a zinc/air battery, the electrode reactions are:

negative electrode

$$Zn(OH)_4^{2-} + 2e^- \underset{\text{discharge}}{\overset{\text{charge}}{\rightleftharpoons}} Zn + 4OH^- \quad (1)$$

positive electrode

$$4OH^- - 4e^- \underset{\text{discharge}}{\overset{\text{charge}}{\rightleftharpoons}} O_2 + 2H_2O \quad (2)$$

battery

$$2Zn(OH)_4^{2-} \underset{\text{discharge}}{\overset{\text{charge}}{\rightleftharpoons}} 2Zn + O_2 + 4OH^- + 2H_2O \quad (3)$$

The battery has an open circuit potential of ~ 1.65 V. Clearly, one requirement is a bifunctional oxygen electrode, ie. an electrode that supports both oxygen evolution and reduction with low overpotentials.

A recent communication [7] described a novel procedure for fabrication of a bifunctional oxygen electrode for alkaline secondary metal air batteries. In this procedure, a nickel metal powder/PTFE gas diffusion electrode (GDE) is preformed within a nickel foam prior to the deposition of a catalyst layer by dip coating and thermal treatment. This paper now reports the influence of the numerous parameters in the fabrication procedure on the performance of these electrodes.

While the choice of electrocatalyst to minimise overpotentials is clearly important, it needs to be recognised that a gas diffusion electrode suitable as a bifunctional oxygen electrode must have a series of additional properties. It must have a structure that provides an effective barrier to crossover of both gas and electrolyte while permitting a high flux of oxygen to the catalyst centres during discharge and release of oxygen to the gas side during charge. Also there must be low resistance, current pathway between catalyst centres and external contacts that prevents IR drops and an uneven current distribution. The target is to design electrodes that have the physical and mechanical properties to allow their scale-up and implementation in flow cells with electrode areas up to 1 m^2.

The design of the GDEs was based on a number of conclusions from preliminary experiments and the literature.

(a) Nickel cobalt spinel, $NiCo_2O_4$ was selected as the electrocatalyst [8-14]. Preliminary experiments showed that it gave overpotentials for both oxygen evolution and reduction that were at least comparable to other electrocatalysts including precious metals. However, it had the advantage that it was prepared in a simple procedure and this could be achieved at a relatively low temperature where other components of the GDEs were stable. This is essential for application of the spinel catalyst after the formation of the gas diffusion layer.

(b) Carbon materials within the GDEs (powder and paper) were avoided since the literature has concluded that carbons corrode under the forcing conditions of oxygen evolution [15-18] and this was also our experience.

(c) The polymer selected as binder in the GDEs was PTFE. Cation conducting polymers were considered unsuitable because of the key role of hydroxide ion in the battery chemistry and no anion conducting polymers with the appropriate properties have been located.

The medium chosen was 8 M NaOH at 333 K. Sodium hydroxide is substantially cheaper than potassium hydroxide and allows a significant increase in the zincate concentration (1.2 M cf 0.5 M). The use of the elevated temperature leads to large decreases in the overpotentials for the electrode reactions as well as increasing the solubility of the sodium zincate; it is also a typical steady state temperature for a large scale electrolysis cell system.

2. Experimental

2.1 Chemicals

Nickel powder (2–10 μm particle size determined by SEM) was supplied by Huizhou Wallyking Battery Ltd, China. Two sources of nickel foam were used - Goodfellow Metals (thickness 1.9 mm, 20 pores/cm) and Changsha Lyrun New Material Co. Ltd (thickness 1.6 mm, 43 pores/cm). Nickel nitrate (Aldrich, 99.999%), cobalt(II) nitrate (Aldrich, ≥ 98%), sodium hydroxide (Fisher, 97%), polytetrafluoroethylene (PTFE, Aldrich, 60 wt% dispersion in H_2O) were used as received.

An electrode prepared from nickel cobalt spinel, $NiCo_2O_4$, powder was used for comparison. The powder was prepared by a thermal decomposition procedure.

$Ni(NO_3)_2.6H_2O$ (14.54 g) and $Co(NO_3)_2.6H_2O$ (29.1 g) were dissolved in methanol (100 cm^3) and heated at 338 K in fume cupboard to evaporate solvent. The dried powder sample was placed into the Carbolite furnace in air at 648 K for 20 hours. The resulting black powder was characterized by SEM, TEM, EDAX, XRD, BET analysis and particle size analysis and a further paper [19] will discuss the data in detail as well as comparing spinel powders from several preparation procedures. Here, we note that samples from repetition of the preparation led to materials with well-defined XRD patterns characteristic of a spinel structure, a ratio of Ni:Co close to 1:2 (determined by both EDAX and elemental analysis), BET surface area of ~10 m^2 g^{-1} and particles sized below 5 μm.

2.2 Preparation of Gas Diffusion Electrodes

The procedure for making the bifunctional oxygen gas diffusion electrodes (GDEs) is illustrated with a particular example. The first stage led to a porous nickel powder/PTFE layer on nickel foam. The nickel foam (a disc, diameter 12 mm) was ultrasonicated in acetone for 20 minutes, acid etched in 1 M HCl at 353 K for ~ 1 hour and then washed with water and ultrasonicated in water for 15 minutes. Nickel powder (150 mg) and 60 % PTFE solution (75 mg) were mixed with isopropanol (0.5 cm^3) and water (0.5 cm^3). The paste was then ultrasonicated for 20 minutes and homogenised for 4 minutes to form an ink before drying to a paste with a ratio of Ni:PTFE of 10:3. The Ni/PTFE paste (200 mg wet weight ~ 120-150 mg dry weight) was spread uniformly over the Ni foam disc and pressed in a Specac hydraulic press at 1.5 kN cm^{-2} and 298 K for 30 s. The second step was to form the catalyst layer. The nickel powder/PTFE coated nickel foam was soaked in a solution containing 1 M $Ni(NO_3)_2$ and 2 M $Co(NO_3)_2$ in 50/50 isopropanol/water, dried at 298 K for ~ 60 s and then heat treated at 648 K in air for 10 min to form the $NiCo_2O_4$ spinel. The dip, dry and heat cycle was repeated 3 times before the sample was calcined at 648 K for 3 hours. The procedure always had the two stages but a number of parameters within it (eg. ratio of Ni:PTFE, loading, dipping solution, thermal treatment) were varied as set out in the results section. For comparison, some GDEs were prepared where $NiCo_2O_4$ spinel powder was used instead of Ni powder; these were fabricated in a single stage.

Figure 1 reports SEM images of the $NiCo_2O_4$ coated Ni powder/PTFE GDEs. Figure 1(a) shows the uniform surface of the electrodes exposed to the electrolyte when mounted in the cell; an SEM images of the gas side clearly show that foam structure is maintained. Figure 1(b) shows a cross section SEM image; there is 50 μm dense layer on the electrolyte side and the fill of the foam decreases away for this surface to give open foam. Figure 2

shows high resolution SEM images of the surface of the $NiCo_2O_4$ coated Ni powder/PTFE GDE along with the Ni/PTFE layer before deposition of the spinel catalyst. It can be seen that before the coating with catalyst, the surface consists of small angular particles of nickel while after coating, rather unstructured, 'fluffy' patches of the spinel catalyst are dispersed over the surface.

2.3 Electrochemical Experiments

Electrochemical experiments were carried out in a water jacketed glass cell (volume 200 cm^3), see figure 3, with a GDE, a platinum gauze counter electrode and a laboratory prepared Hg/HgO reference electrode placed inside a compartment with a Luggin capillary. The GDE disc (diameter 12 mm) was mounted inside a PTFE holder, see figure 3(b) with the $NiCo_2O_4$ coated Ni powder/PTFE layer adjacent to the electrolyte. The area of the GDE exposed to the electrolyte was 0.5 cm^2 and electrical contact was made with a circle of Ni wire around the perimeter of the disc on the gas side. A Grant TC120 recirculator with 5 litre reservoir maintained the electrolyte temperature at 333 K. O_2 was passed to the rear of the GDE with a feed rate of 200 cm^3 min^{-1}, controlled via a flow meter. The electrolyte was 8 M NaOH at 333 K. Current cycling was carried out under galvanostatic control at current densities in the range 10 – 100 mA cm^{-2}. All current densities are based on the geometric area of the electrode (0.5 cm^2) exposed to the electrolyte and gas compartments. Electrochemical measurements were carried using an Autolab potentiostat/galvanostat, PGSTAT128N.

2.4 Other Instrumentation

SEM images and EDAX data were obtained on a JSM 6500F Scanning Electron Microscope. Powder XRDs were recorded on an Agilent Supernova XRD Diffractometer with a Mo kα source. A small sample of powder was prepared in a 0.3 mm diameter glass capillary. Theoretical $NiCo_2O_4$ pattern produced using Crystal Maker v8.7.2 and Crystal Diffract v5.2. Surface areas were determined with a Micromeritics – Gemini BET Instrument using nitrogen as the gas.

3 Results and Discussion

Initially, the performance of a $NiCo_2O_4$ coated Ni powder/PTFE GDE and a $NiCo_2O_4$ powder/PTFE GDE during both O_2 reduction and O_2 evolution were compared in 8 M NaOH and at a temperature of 333 K. In these experiments, a cathodic current was passed for 30 minutes, then an anodic current for the same period (corresponding to discharging and charging of a battery respectively) and the potential of the GDEs *vs* a Hg/HgO reference

electrode were recorded. Figure 4 shows the responses for three current densities. It can be seen that following a short initial period, the potentials are always constant. Also the difference in potentials for O_2 reduction and evolution increase slightly with current density due to increases in the overpotentials and IR drops. Clearly, there are significant overpotentials associated with both O_2 reduction and evolution but the differences in potential between the two reactions, 710 mV and 770 mV for the spinel powder and spinel coated Ni electrodes respectively at 50 mA cm^{-2}, compares favourably with all other catalysts tested and this included a number containing precious metals. It can also be seen that the spinel powder electrodes performed slightly better than the spinel coated Ni GDEs but the difference in performance decreased with increasing current density. The improvement in performance is, however, achieved at the cost of a very heavy loading of spinel catalyst. Hence, electrodes were prepared with mixtures of nickel metal and spinel powders, followed by dip coating and some results are summarised in table 1. The overpotentials for both O_2 reduction and evolution decrease as the spinel content is increased but even 10% spinel corresponds to a high weight loading of catalyst. Hence, since a significant improvement in performance requires a high loading of spinel powder, the electrodes based on Ni powder have been developed further.

It was shown in an earlier communication [7] that O_2 evolution and reduction occur with the transition metals ions within the spinel structure in different oxidation states. This leads to a different open circuit potential following reduction or evolution and to the initial periods before the potential takes up a constant value when the electrode is switched between O_2 evolution and reduction (see figure 4). The first reaction to occur is always the change in oxidation state of the metals ions within the spinel before the O_2 reactions take over when the spinel is full oxidised/reduced. As expected the initial period is most pronounced with higher spinel content (powder *vs* coating) and lower current density.

Table 1 also reports the behaviour of a Ni powder/PTFE GDE that has not been subjected to the second stage of the fabrication procedure, ie. dip coating and heat treatment to form a spinel coating. The resulting GDE is a very bad electrode for O_2 reduction. In the steady state with a cathodic current, the potential takes up a value close to – 1000 mV *vs* Hg/HgO with the major reaction occurring being H_2 evolution. The $NiCo_2O_4$ layer is the catalyst for the O_2 reactions and a key component of the bifunctional GDEs.

The conditions for the formation of the spinel coating in the GDEs were investigated. In all cases, the thermal treatment was carried out at 648 K for 3 hours since $NiCo_2O_4$ is formed rapidly at this temperature and thermogravimetric analysis showed that PTFE underwent decomposition above 670 K. Indeed, the fact that the spinel is formed at a relatively low temperature where the PTFE is chemically stable is a key factor in the choice of the catalyst for these GDEs. The temperature of 648 K is, however, certainly sufficient to cause the polymer to flow and the heat treatment is likely to be influential in determining the final structure of the GDEs. Firstly, GDEs were prepared using several different nickel and cobalt salts dissolved in water and the results are presented in table 2. The significant difference is in the potential for the reduction reaction since the nickel foam substrate is already a reasonable catalyst for O_2 evolution. The temperature of the thermal treatment is insufficient to convert the chloride material to the spinel structure but both the acetates and the nitrates are converted to effective catalyst and the latter were used in all later preparations. Secondly, the total concentration of the Ni/Co nitrate solution in the dip solution was varied (0.75, 1.5 and 3 M) while maintaining the Ni:Co ratio at 1:2. The overpotentials for both O_2 reduction and evolution were reduced using the more concentrated solution; GDEs prepared with the 3 M solution gave a potential gap between O_2 reduction and evolution ~ 100 mV less than GDEs prepared with the 0.75 M solution with a current density of 50 mA cm^{-2}. Finally, the influence of the solvent for the dip solution was studied. Solutions of the Ni/Co nitrates were prepared in 1:1 mixtures of water with five alcohols. The alcohols led to small improvements in the performance of the GDEs probably resulting from changes in surface tension and/or viscosity leading to differences in the ability of the dip solution to diffuse into the Ni powder/PTFE layer. The 1:1 isopropanol:water dip solution led to a GDE with the smallest difference in potential between O_2 reduction and evolution. With the 1:1 isopropanol:water solution containing 3 M Ni/Co nitrates, three dip/thermal treatment cycles were sufficient to give the optimum GDE performance when the spinel catalyst loading was estimated by weight change as ~ 3 mg cm^{-2}.

The ratio of PTFE binder to nickel powder is expected to be a key factor in determining the performance of the GDEs, particularly the stability of performance during extended operation. Electrodes with PTFE contents between 12 % and 27 % were therefore tested. All the GDEs initially supported both reactions. Figure 5 reports the separation of the potentials for O_2 evolution and reduction as a function of PTFE content; the data is taken from the initial charge/charge cycles at 50 mA cm^{-2}. At the extremes of this range, it was

difficult to obtain reproducible data but over the range 18 – 23% electrodes could be fabricated reproducibly and the separation of the potentials for O_2 evolution and reduction varied little. The problem at low PTFE content was entry of the electrolyte into the porous structure and this became more obvious with cycling of the electrodes – the potential difference between O_2 evolution and reduction increased and on dismantling the cell, electrolyte could be seen on the gas side. With PTFE content above 23 %, the potential difference was higher either because of hindered access of gas or electrolyte to the catalyst centres or an increase in the resistance of the electrodes. Hence, long term stability without a large increase in the potential difference was considered critical, 23 % PTFE (ratio of Ni powder:PTFE = 10:3) was selected as the safe option.

Further sets of experiments were carried out to define the influence of the weight loading of Ni powder/PTFE (10:3) paste and the pressure exerted during the manufacture of the GDEs. In the first set the loading was varied over the range 120 - 280 mg cm^{-2} of wet paste. The lowest loading suffered from electrolyte leakage through to the gas side but over the range 140 - 280 mg cm^{-2} good responses were obtained, see figure 6, with a small trend to higher overpotentials with thickening of the Ni powder/PTFE layer. Electrodes were also pressed with compressions in the range 0.5 – 2.5 kN cm^{-2}; the lowest pressure was insufficient to create a compact electrodes and leakage was an immediate problem, but above 1 kN cm^{-2} the electrodes gave good data with a slight tendency for the overpotentials to increase with increasing pressure (see figure 7), probably due to a decrease in size of the gas pores. Electrodes prepared with a loading of 200 mg cm^{-2} wet paste (approximately 90 mg cm^{-2} Ni + 30 mg cm^{-2} PTFE) and a compression of 1.5 kN cm^{-2} showed reproducible behaviour and good long term stability and have been used for further electrode development.

Several electrodes were further tested by cycling 10 times between 30 minutes O_2 reduction and 30 minutes O_2 evolution using current densities of 20 mA cm^{-2} or 50 mA cm^{-2}. In general, stable potentials were observed each cycle following initial periods where the spinel coating is oxidised/reduced and commonly the potentials for O_2 reduction and O_2 evolution were unchanged during the 10 cycles. Some electrodes, eg. those with a low PTFE content, showed a small negative shift in the potential during O_2 reduction over the 10 cycles and this was taken as an indication of ingress of aqueous electrolyte into the GDE structure reducing the access of O_2 gas to the catalyst sites.

In the literature, air is preferred to oxygen as the cell feed when batteries are discharged. Although the possibility exists for storing and using the pure O_2 evolved during charge (and this avoids CO_2 degradation of the alkaline electrolyte when non-purified air is employed), some tests employed an air feed. The responses during charge/discharge cycling were similar in shape and stable potentials were established but the potential for oxygen reduction shifted negative. At 50 mA cm^{-2}, the negative shift was 70 mV.

These carbon free GDEs also met the requirement that during charge the oxygen was evolved into the gas phase and away from the interelectrode gap. While a continuous and rapid stream of fine H_2 gas bubbles can be seen leaving the Pt mesh cathode, no O_2 gas bubbles appear at the GDE/electrolyte interface. Hence, while with the present equipment, any small fraction of the O_2 entering the electrolyte cannot be quantified, it is clear that almost all the O_2 is released to the back of the GDE.

Although the glass cell and auxiliary equipment used in this programme were not designed for testing over many days, some longer term experiments have been carried out. Figure 8 shows the potential *vs* time responses for cycles 1 – 10 and 40 - 50 for an experiment carried out with a current density of 50 mA cm^{-2} and fabricated using the precise conditions of the recipe in the Experimental Section. It can be seen that there is a slight trend to an improvement in performance with cycling but the changes in the potentials over the 50 cycles are small. The average separation of the potentials for O_2 reduction and evolution during the 50 cycles is 800 mV. Such performance in a Zn/air battery is equivalent to a voltage efficiency ~ 60 %. In fact, the experiment was continued for 100 cycles but beyond 50 cycles, the potential for O_2 reduction became more negative with time, reaching -440 mV after 100 cycles.

Larger GDEs have been fabricated. 100 mm x 100 mm electrodes made from the thinner Ni foam have been tested in a flow cell. These larger electrodes are flat with a uniform black appearance and their thickness was measured as 0.75 mm. They are also robust and can be extensively handled without damage making them well suited to incorporation into flow cells.

4. Conclusions

Gas diffusion electrodes without carbon components have been satisfactorily fabricated and tested as a bifunctional electrode for O_2 reduction/evolution. The electrodes

can operate at 100 mA cm^{-2} and cycle well at 50 mA cm^{-2} and the performance may well be adequate for practical secondary Zn/air batteries. These current densities are, however, low compared to those possible with MEA type GDEs with carbon components for fuel cells (> 1000 mA cm^{-2}) suggesting that further enhancement of the O_2 flux is still possible. Moreover, the overpotentials observed for both O_2 reduction and O_2 evolution, while comparable with those reported for other catalysts, are not as low as one would like. The choice of $NiCo_2O_4$ spinel as the catalyst results from the fact that for this method of fabrication of the GDEs, the catalyst layer must be prepared at a temperature below that where the PTFE decomposes.

5. Acknowledgement

Financial support by the European Commission (Theme 2010.7.3.1) *Energy Storage Systems for Power Distribution* Networks, Grant Agreement No. 256759, is gratefully acknowledged.

6. References

1. P. Leung, X. Li, C. Ponce de Leon, L. Berlouis, C.T.J. Low and F.C. Walsh, Progress in Redox Flow Batteries, Remaining Challenges and Their Applications in Energy Storage, *RSC Advances*, (2012) 1-32.
2. Z. Yang, J. Zhang, M.C.W.Kintner-Meyer, X. Lu, J.P. Lemmon and J. Lui, Electrochemical Energy Storage for Green Grid, *Chem. Rev.*, **111** (2011) 3577-3613.
3. M. Skyllas-Kazacos, M.H. Chakrabarti, S.A. Hajimolana, F.S. Mjalli and M. Saleem, Progress in Flow Battery Research and Development, *J. Electrochem. Soc.*, **158** (2011) R55-R79.
4. R.P. Hamlen, T.B. Atwater, in: D. Linden, T.B. Reddy (Eds.), *Handbook of Batteries*, third ed., McGraw-Hill, New York, 2002, pp. 38.1-38.53.
5. F. Cheng and J. Chen, Metal Air Batteries: From Oxygen Reduction Electrochemistry to Cathode Catalysts, *Chem. Soc. Rev*., **41** (2012) 2172-2192.
6. J. Pan, L. Ji, Y. Sun, P. Wan, J. Cheng, Y. Yang and M. Fan, Preliminary Study of Alkaline Single Flowing Zn–O_2 Battery, *Electrochem. Commun.*, **11** (2009) 2191-2194.
7. X. Li, D. Pletcher, A.E. Russell, F.C. Walsh, R.G.A. Wills, S.F. Gorman, S.W. Price and S.J. Thompson, A Novel Bifunctional Oxygen GDE for Alkaline Secondary Batteries, *Electrochem. Commun.*, **34** (2013) 228.

8. K. Kinoshita, *Electrochemical Oxygen Technology*, John Wiley & Sons Inc. 1992.
9. L. Jörissen, Bifunctional Oxygen/Air Electrodes, *J. Power Sources,* 155 (2006) 23-32.
10. M.R. Tarasevich, B.N. Efremov, in: S. Trasatti (Ed.), *Electrodes of Conductive Metallic Oxides*, Elsevier Scientific Publishing Company, 1980, pp. 221-59.
11. P. Rasiyah, A.C.C. Tsueng, D.B. Hibbert, A Mechanistic Study of Oxygen Evolution on $NiCo_2O_4$. 1. Formation of Higher Oxides, *J. Electrochem. Soc*., **129** (1982) 1724-1727.
12. P. Rasiyah and A.C.C. Tseung, A Mechanistic Study of Oxygen Evolution on $NiCo_2O_4$. 2. Electrochemical Kinetics, *J. Electrochem. Soc*., **130** (1983) 2384-2386.
13. P.N. Ross, *Proceedings of the 10th Annual Battery Conference on Applications and Advances,* 1995, pp. 131.
14. X. Li, F.C. Walsh and D. Pletcher, A Comparison of Nickel Based Electrocatalysts for Oxygen Evolution in a Zero Gap Water Electrolyser with a Hydroxide Conducting Membrane, *Phys. Chem. Chem. Phys*. 13 (2011) 1162-1167.
15. N. Staud, and P.N. Ross, The Corrosion of Carbon Black Anodes in Alkaline Electrolyte, Part II. Acetylene Black and the Effect of Oxygen Evolution Catalysts on Corrosion, *J. Electrochem. Soc.,* **133** (1986) 1079-1084.
16. P.N. Ross and M. Sattler, The Corrosion of Carbon Black Anodes in Alkaline Electrolyte, Part III. The Effect of Graphitization on the Corrosion Resistance of Furnace Blacks, *J. Electrochem. Soc.,* **135** (1988) 1464-1470.
17. N. Staud, H. Sokol and P.N. Ross, The Corrosion of Carbon Black Anodes in Alkaline Electrolyte, Part IV. Current Efficiencies for Oxygen Evolution from Oxide-Impregnated Graphitized Furnace Blacks, *J. Electrochem. Soc.,* **136** (1989) 3570-3576.
18. S. Műller, F. Holzer, H. Arai and O. Haas, A Studyof Carbon-Catalyst Interaction in Bifunctional Air Electrodes for Zinc-Air Batteries, *J. New Mater. Electrochem. Systems,* **2** (1999) 227-232.
19. S.W. Price, S.J. Thompson, D. Pletcher and A.E. Russell, *to be published.*

Sample	Dip Coated	Reduction E/ mV *vs* Hg/HgO	Evolution E/ mV *vs* Hg/HgO	ORR-OER Gap, Δ*E*/mV
100 % Ni	No	H_2 evolution	***	-
100% Ni	Yes	-208	658	866
90% Ni/10% $NiCo_2O_4$	Yes	-183	628	811
50% Ni/50% $NiCo_2O_4$	Yes	-166	589	755
100% $NiCo_2O_4$	Yes	-138	532	670

Table 1 *Potentials for O_2 reduction and evolution at 50 mA cm^{-2} for GDEs prepared with Ni powder (dip coated with $NiCo_2O_4$ and also without dip coating), spinel and mixtures of nickel and spinels (dip coated). GDEs were 10:3 Ni powder:PTFE and the spinel coating was formed at 648 K for 3 hours. 8 M NaOH. 333 K.*

Salt	O_2 Reduction E/ mV *vs* Hg/HgO	O_2 Evolution E/ mV *vs* Hg/HgO	ORR-OER Gap, Δ*E*/mV
Nitrate	-125	594	719
Sulphate	-378	575	953
Chloride	-1068	526	1594
Acetate	-149	600	749

Table 2 *Influence of the anion of the nickel and cobalt salts used in the dip coating solution on performance. GDEs were 10:3 Ni powder:PTFE and the spinel coating was formed at 648 K for 3 hours. Constant current experiments carried at 20 mA cm^{-2} in 8 M NaOH at 333 K.*

Legends to Figures

Figure 1

SEM images of the bifunctional GDE (a) the surface of the spinel coated Ni powder/PTFE layer and (b) a cross section of the electrode.

Figure 2

High resolution SEM images of the surfaces of the bifunctional GDE (a) Ni powder/PTFE layer before coating with catalyst (b) $NiCo_2O_4$ coated Ni powder/PTFE layer.

Figure 3

Schematic of the three electrode cell used together with an expansion of the GDE structure.

Figure 4

Comparison of the performance of a $NiCo_2O_4$ coated Ni powder/PTFE GDE and a $NiCo_2O_4$ powder/PTFE GDE during O_2 reduction and O_2 evolution. Potential vs time plots at (a) 20 mA cm^{-2} (b) 50 mA cm^{-2} and (c) 100 mA cm^{-2}. 8 M NaOH. 333 K.

Figure 5

The influence of the PTFE content on the performance of $NiCo_2O_4$ coated Ni powder/PTFE GDEs for O_2 reduction and O_2 evolution at 50 mA cm^{-2} - difference in potentials for O_2 reduction and O_2 evolution vs % PTFE. 8 M NaOH. 333 K.

Figure 6

Plots of potential versus time for $NiCo_2O_4$ coated Ni powder/PTFE GDEs during O_2 reduction and O_2 evolution at 20 mA cm^{-2}as a function of the loading with Ni powder/PTFE (10:3) paste. 8 M NaOH. 333 K.

Figure 7

Influence of compression during $NiCo_2O_4$ coated Ni powder/PTFE GDE preparation on O_2 reduction, O_2 evolution cycling at 50 mA cm^{-2}. 8 M NaOH, 333K, 200 ml min^{-1} O_2,

Figure 8

Potential vs time responses during current density cycling of a $NiCo_2O_4$ coated Ni powder/PTFE GDE at 50 mA cm^{-2} in 8 M NaOH at 333 K. Oxygen feed rate: 200 cm^3 min^{-1}. Shown are 1-10 and 40-50 cycles.

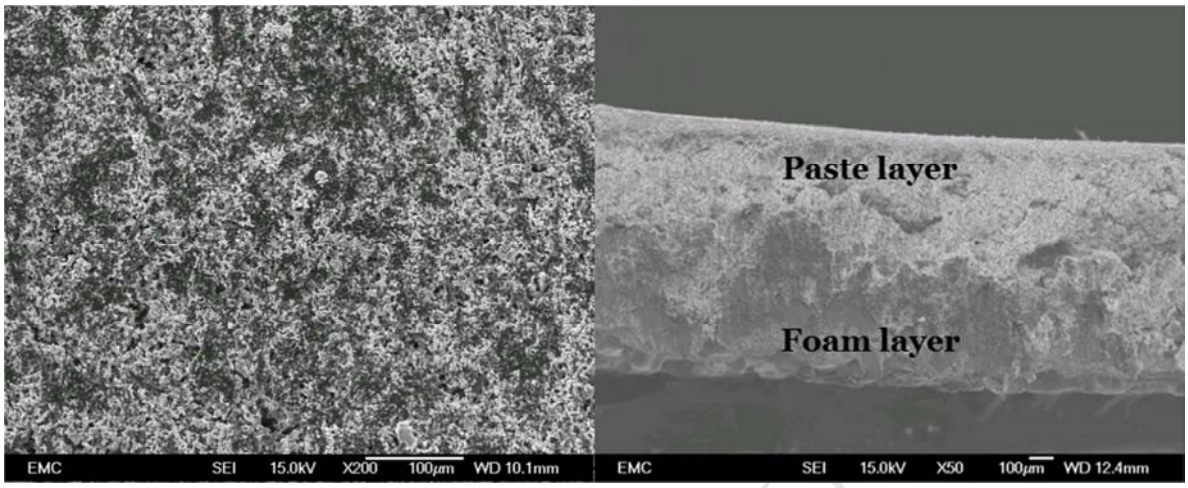

(a) (b)

Figure 1 *SEM images of the bifunctional GDE (a) the surface of the spinel coated Ni powder/PTFE layer and (b) a cross section of the electrode.*

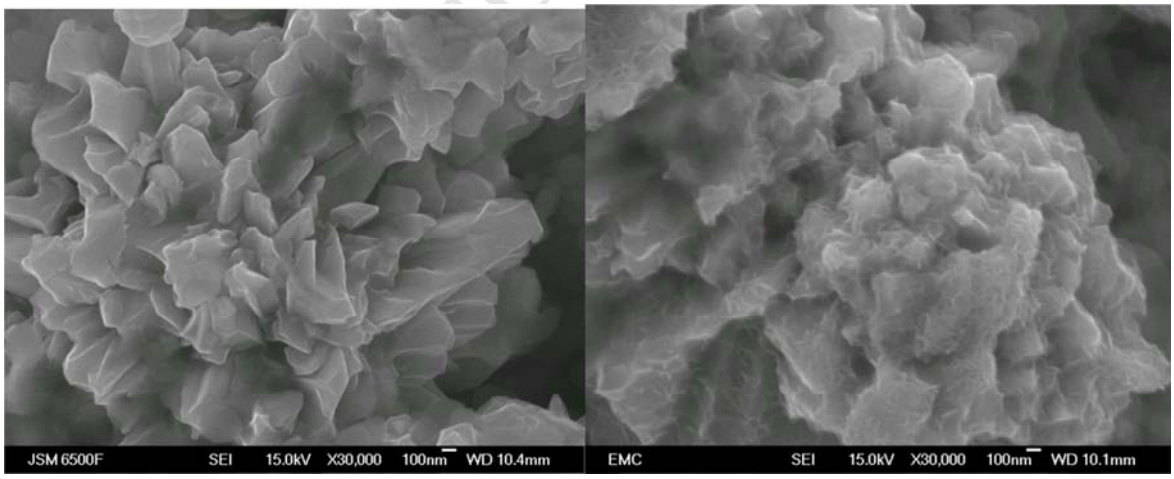

Figure 2 *High resolution SEM images of the surfaces of the bifunctional GDE (a) Ni powder/PTFE layer before coating with catalyst (b) $NiCo_2O_4$ coated Ni powder/PTFE layer.*

(a)

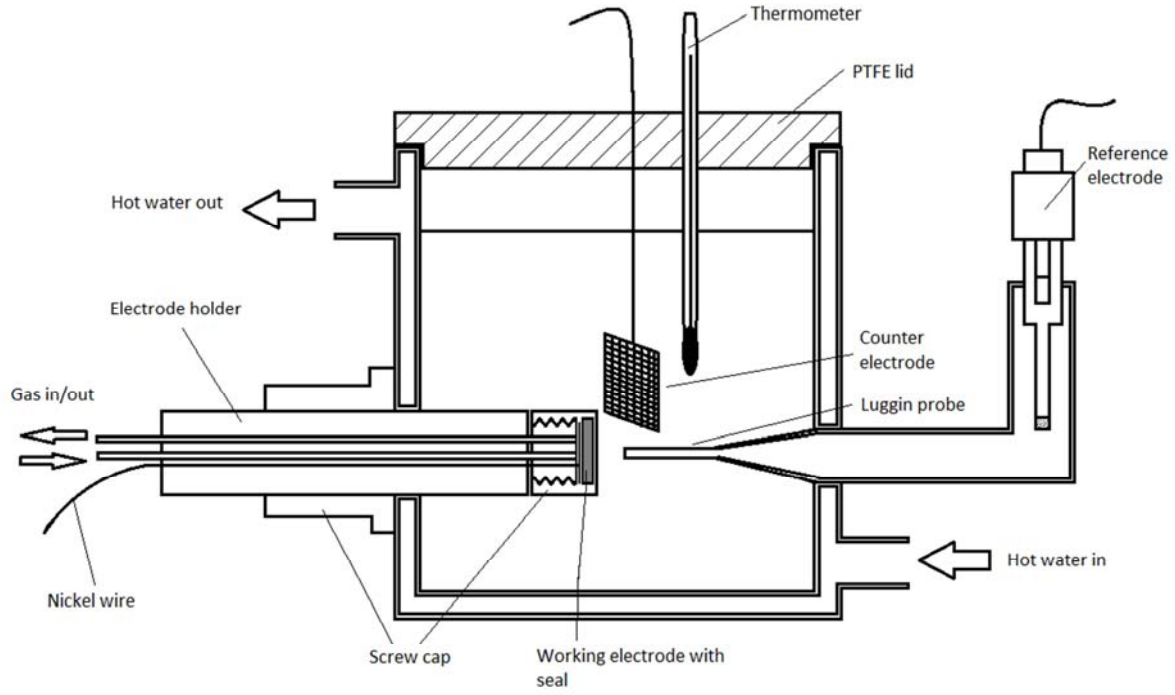

(b)

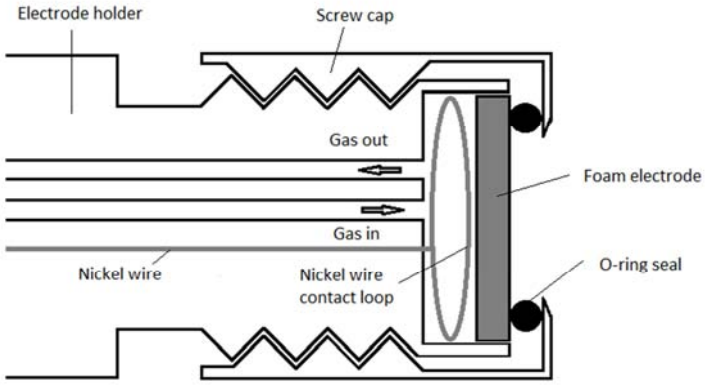

Figure 3 *Schematic of the three electrode cell used together with an expansion of the GDE structure.*

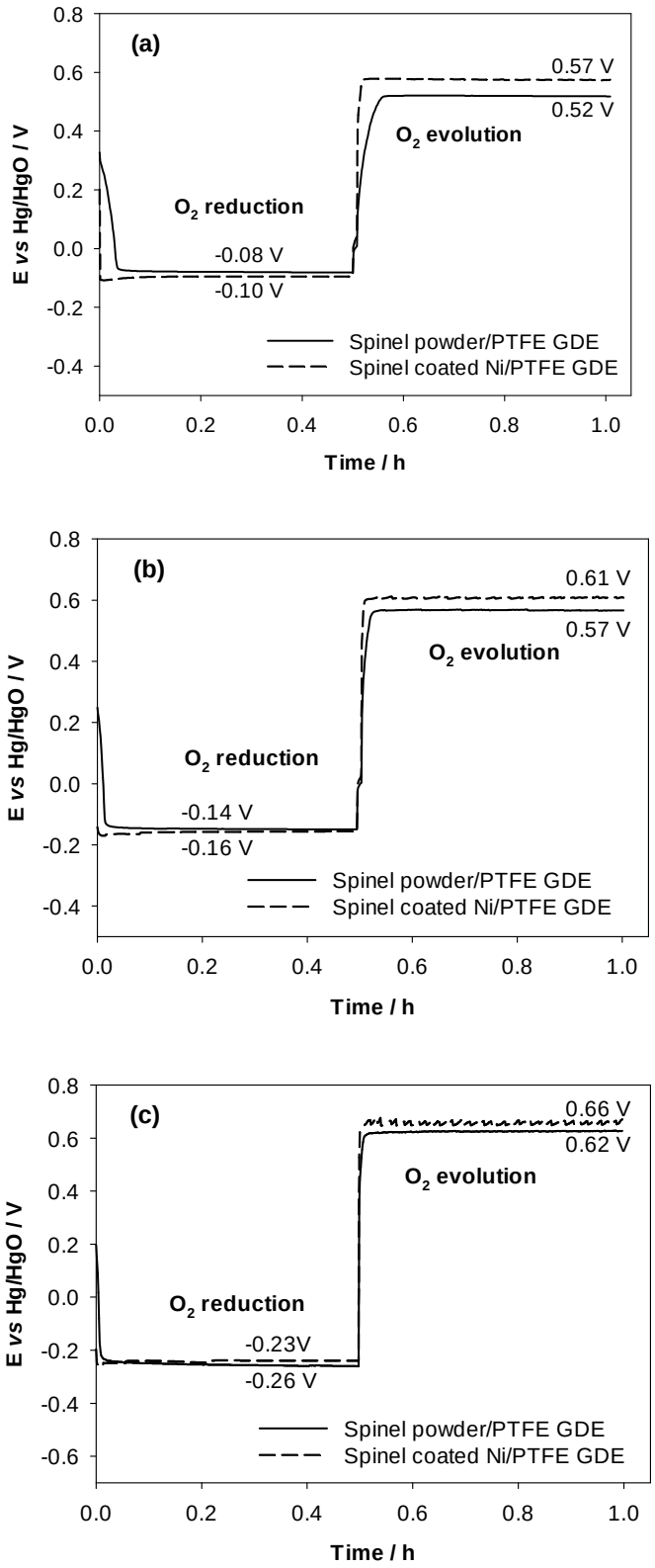

Figure 4 *Comparison of the performance of a $NiCo_2O_4$ coated Ni powder/PTFE GDE and a $NiCo_2O_4$ powder/PTFE GDE during O_2 reduction and O_2 evolution. Potential vs time plots at (a) 20 mA cm^{-2} (b) 50 mA cm^{-2} and (c) 100 mA cm^{-2}. 8 M NaOH. 333 K.*

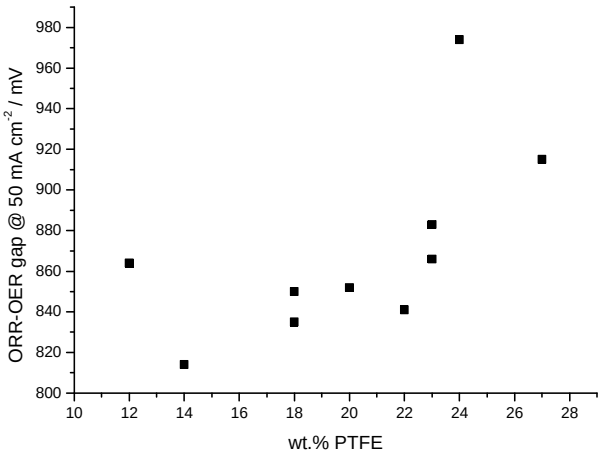

Figure 5 *The influence of the PTFE content on the performance of $NiCo_2O_4$ coated Ni powder/PTFE GDEs for O_2 reduction and O_2 evolution at 50 mA cm^{-2} - difference in potentials for O_2 reduction and O_2 evolution vs % PTFE. 8 M NaOH. 333 K.*

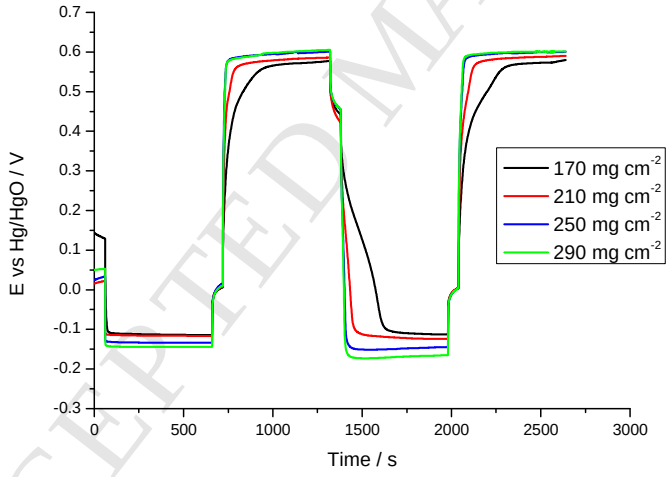

Figure 6 *Plots of potential versus time for $NiCo_2O_4$ coated Ni powder/PTFE GDEs during O_2 reduction and O_2 evolution at 20 mA cm^{-2} as a function of the loading with Ni powder/PTFE (10:3) paste. 8 M NaOH. 333 K.*

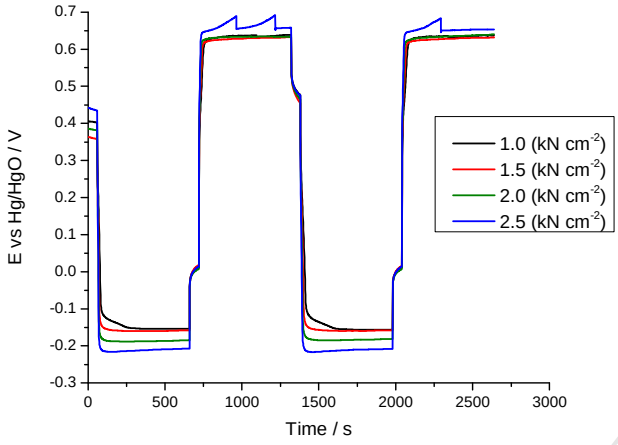

Figure 7 *Influence of compression during $NiCo_2O_4$ coated Ni powder/PTFE GDE preparation on O_2 reduction, O_2 evolution cycling at 50 mA cm^{-2}. 8 M NaOH, 333K, 200 ml min^{-1} O_2,*

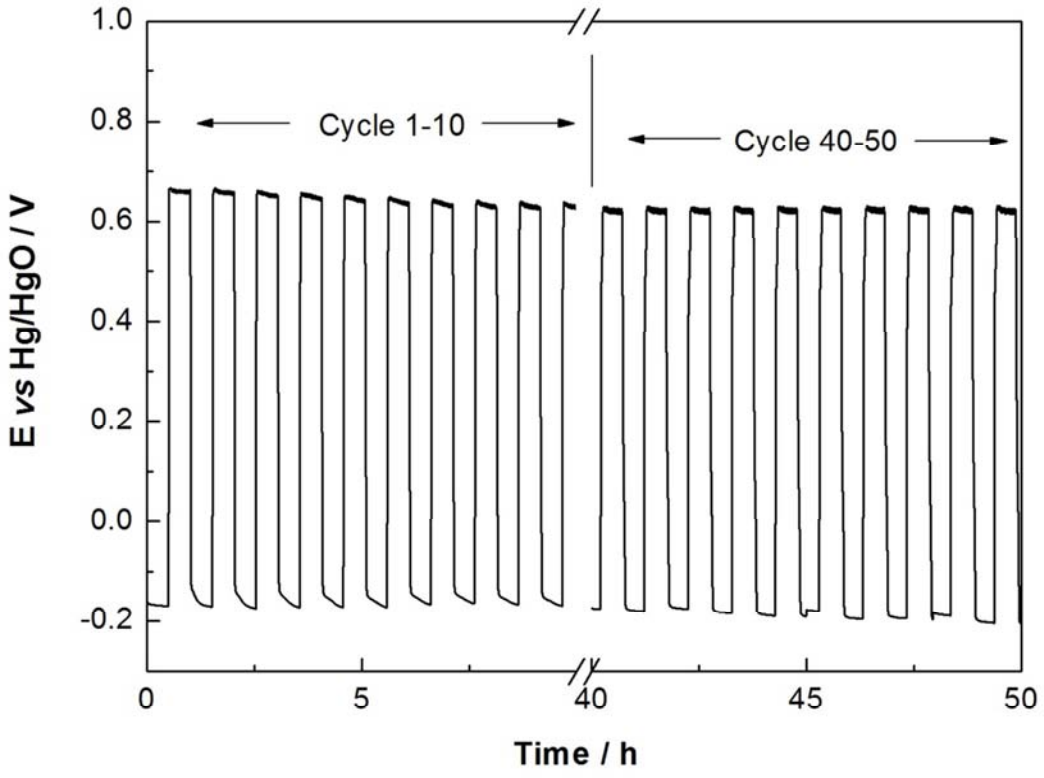

Figure 8 *Potential vs time responses during current density cycling of a $NiCo_2O_4$ coated Ni powder/PTFE GDE at 50 mA cm^{-2} in 8 M NaOH at 333 K. Oxygen feed rate: 200 cm^3 min^{-1}. Shown are 1-10 and 40-50 cycles.*

Highlights:

The Fabrication of a Bifunctional Oxygen GDE without Carbon Components for Alkaline Secondary Batteries

- Fabrication and development of a carbon free bifunctional gas diffusion electrode
- Good stability and overpotentials on cycling at 50 mA cm^{-2} for >50 cycles
- Operational up to current densities of 100 mA cm^{-2}